

Ultimate Stress of the Steel Tube in Circular CFT Stub Columns Subjected to Axial Compression

Siqi Lin and Yan-Gang Zhao

Abstract—Concrete-filled steel tube column achieves excellent performance of high strength, stiffness and ductility due to the confinement effect from the steel tube. Well understanding the stress of the steel tube is important to make clear the confinement effect. In this paper, the ultimate stress of the steel tube in circular concrete-filled steel tube columns subjected to axial compression was studied. Experimental tests were conducted to investigate the influences of the parameters of the column, including concrete strength, steel strength, and D/t ratio, on the ultimate stress of the steel tube. The stress of the steel tube is determined by the Prandtl-Reuss flow rule associated with isotropic strain hardening. Results indicate that the stress of steel tube was influenced by the parameters. Steel tube in the specimen with higher strength ratio f_y/f_c and/or smaller D/t ratio generally exhibits a higher strain hardening behavior, thus leading to a higher utilization efficiency of the steel tube.

Index Terms—Ultimate stress of the steel tube, CFT stub columns, experimental tests.

I. INTRODUCTION

The construction of high-rise buildings, bridges and subway platforms. The restraining effect of the concrete can either prevent or at least delay local buckling of the steel tube. Moreover, confinement resulting from the steel tube increases the strength of the concrete. This mutual interaction between concrete and steel tube makes CFT column exhibit an excellent performance of high strength, good ductility, high energy absorption capacity, and rapid construction [1], [2].

The composite action between the steel tube and the concrete is the key issue to understand the behavior of concrete-filled tubular members [3]. Extensive studies have been conducted to understand the behavior of the CFT columns resulting from the composite action [4]—[10]. Previous studies confirmed that the enhancement of structural properties in CFT columns is due to the composite action between the constituent elements [11]. Several observations can be made from the results of previous studies: (1) Good confinement effect is provided by the steel tube for specimen with small D/t ratio, which lead to improvements in concrete strength and ductility, and more favorable post-yield behavior of the specimen [4], [5],[9]; (2) Confinement was found more effective when the steel tube was filled with ordinary strength concrete(OSC), due to its higher deformation capacity in comparison with the high strength concrete (HSC) [12], [13].

Manuscript received August 7, 2017; revised March 12, 2018.

Siqi Lin and Yan-gang Zhao are with the Dept. of Architecture and Building Engineering, Kanagawa University, Yokohama, 2218686 Japan (e-mail: lsq8986@gmail.com, zhao@kanagawa-u.ac.jp).

Improvements in concrete strength and ductility were observed marginal for specimens filled with very high strength concrete [5]; (3) The use of steel tube with high yield stress in CFT columns is generally believed not necessary due to that increasing steel strength has a minimal effect on improving concrete ductility or strength [10].

Composite effect makes steel tube subjected to a complicated biaxial stress state. An elastic-perfectly-plastic theory with associated flow rule is generally adopted to model the steel tube in the analysis of CFT columns [6], [10], [14]–[16], which actually assumes the steel tube yielded and ignores the strain hardening of the steel tube [15]. However, it is known that ultimate stress of the steel tube could vary remarkably under different composite effects. As for the thin-walled high strength concrete filled steel tube column, the ultimate stress of the steel tube may not reach the yield stress; On the other hand, as for the thick-walled normal strength concrete-filled steel tube column, the steel tube may experience a significant strain-hardening behavior. A large hoop tensile stress can be developed in the strain hardening process and pushes outward the ‘Von Mises’ yield surface [17]. It was found that the structural behaviors of the CFT columns cannot be well predicted for not considering the strain hardening of the steel tube [18]. Choi and Xiao [16] suggested that the strain hardening or softening of the materials should be included to develop a more sophisticated tool to analyze the behavior of the CFT columns. Moreover, it is known that the stress of the steel tube determines the lateral confining stress of the concrete, which significantly influences the axial capacity of a CFT column [15]. Therefore, clearly probing into the stress state of the steel tube is the key to understand the behavior of the column and accurately predict the axial capacity, to which, however, few attentions have been paid so far. Thus, the object of this paper is to investigate the ultimate stress of the steel tube in CFT stub columns based on the experimental tests subjected to axial compression.

II. EXPERIMENTAL TEST TO INVESTIGATE THE ULTIMATE STRESS OF THE STEEL TUBE

A. Determination of the Stress of the Steel Tube

Experimental tests were conducted to investigate the stress of the steel tube in CFT columns. The axial stress and hoop stress of the steel tube are determined from the strains measured in the experimental tests, as summarized below.

The von Mises stress (or the equivalent stress) is used to determine the stress state of the steel tube:

$$\sigma_e = \sqrt{\sigma_z^2 - \sigma_z \sigma_\theta + \sigma_\theta^2}. \quad (1)$$

In the elastic stage, the stress of the steel tube is calculated by the generalized Hooke law. Since the steel tube, as a thin-walled structure, is generally considered under a state of plane stress, the stress of the steel tube could be determined by:

$$\begin{cases} d\sigma_z \\ d\sigma_\theta \end{cases} = \frac{E_s}{1-\nu^2} \begin{bmatrix} 1 & \nu \\ \nu & 1 \end{bmatrix} \begin{cases} d\varepsilon_z \\ d\varepsilon_\theta \end{cases} \quad (2)$$

where $d\varepsilon_z$ and $d\varepsilon_\theta$ are the incremental axial strain and hoop strain, respectively. Poisson ratio and the tangent modulus [19] are given, respectively, by:

$$\nu = \begin{cases} 0.283 & \sigma_e < f_p \\ 0.217 \frac{\sigma_e - f_p}{f_y - f_p} + 0.283 & f_p \leq \sigma_e \leq f_y \\ 0.5 & \sigma_e > f_y \end{cases} \quad (3)$$

$$E_s = \begin{cases} E & \sigma_e < f_p \\ \frac{(f_y - \sigma_e)\sigma_e}{(f_y - f_p)f_p} E & f_p \leq \sigma_e \leq f_y \end{cases} \quad (4)$$

where f_p is the proportional limit, taken herein to be $0.75f_y$.

In the plastic stage, the stress of the steel tube is calculated by the incremental Prandtl-Reuss equation:

$$\begin{cases} d\sigma_z \\ d\sigma_\theta \end{cases} = \frac{E}{1-\nu^2} \begin{bmatrix} 1 & \nu \\ \nu & 1 \end{bmatrix} \begin{cases} d\varepsilon_z \\ d\varepsilon_\theta \end{cases} \quad (5)$$

$$- \frac{Ed\gamma}{3(1-\nu^2)} \begin{bmatrix} 2-\nu & 2\nu-1 \\ 2\nu-1 & 2-\nu \end{bmatrix} \begin{cases} \sigma_z \\ \sigma_\theta \end{cases} \quad (6)$$

$$d\gamma = \frac{9G(s_z d\varepsilon_z + s_r d\varepsilon_r + s_\theta d\varepsilon_\theta)}{2\sigma_e^2(H+3G)} \quad (7)$$

where e_i and s_i are the deviatoric strain and stress, respectively; H is the slope of equivalent stress–equivalent plastic strain curve, which is taken as the slope of the stress–plastic strain curve of the steel from tensile tests; G is the shear modulus.

B. Experimental Program

A total of 24 CFT stub columns were tested under axial compression to investigate the stress of the steel tube. In order to achieve different stress states of the steel tube in CFT columns, a wide range of parameters were carefully designed, including: (1) Nominal tensile strengths of steel F_s : 400 Mpa and 490 Mpa; (2) Concrete design strength F_c : 24Mpa, 36 Mpa, 48 Mpa and 60 Mpa; (3) Ratio of column diameter to steel thickness D/t : 31,65 and 100. All specimens were three times the diameter in length. Two specimens are tested for each kind of columns. For convenience, the CFT column specimen was identified as: F_s - F_c - D/t . Letter of a or b after the identification is the specimen number.

TABLE I: PROPERTIES OF THE SPECIMENS

Specimen	D /mm	t /mm	f_y /Mpa	f_t /Mpa
400- F_c -31	140	4.5	374.2	457.3
490- F_c -31	140	4.5	462.9	547.3

400- F_c -65	208	3.2	360.8	460.4
400- F_c -100	230	2.3	360.8	460.4

The mechanical properties of the steel were obtained from tensile tests of the coupons taken from each steel plate before manufacturing. The 0.2% proof stress is taken as the yield strength of the steel, which for specimens of 400- F_c -31 and 490- F_c -31 are 374.2 Mpa and 462.9 Mpa, respectively, while for specimens of 400- F_c -65 and 400- F_c -100 is 360.8 Mpa. Corresponding tensile strengths of the steels is identified by f_t . Details of the test results are given in table I. The compressive strengths of the concrete f_c for all the specimens are obtained from the compression test of 100×200mm concrete cylinders. It should be noted that although a same design concrete strength is used, slightly different test results of the compressive strength were obtained for some specimens. Compressive strength of the concrete for specimen 400-24-31 is 28.4 Mpa, while for specimens of 400-24-65 and 400-24-100 are 32 Mpa, and for specimen 400-60-31 is 68 Mpa, while for specimens of 400-60-65 and 400-60-100 are 64 Mpa.



Fig. 1. Polishing process.

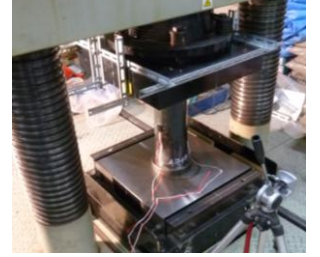


Fig. 2. Experimental test setup.

To provide a flat column end for ensuring that the load is applied evenly to the entire section, all the specimens are polished by a polishing machine. The polishing process is shown in Fig.1. Specimens were subjected to axial monotonic compression under a universal testing machine with a maximum capacity of 5000 kN. The load was applied to the section of the concrete core and the steel tube simultaneously. Longitudinal deformation of the column was read directly from the test machine. Two pairs of electrical strain gauges were placed at the mid-height of the exterior of the steel tube to measure axial and lateral strains of the steel tube. Details of the experimental test setup is shown in Fig. 2.

III. RESULTS AND DISCUSSIONS

A. Relation of Axial Stress-Displacement

The axial stress of the column is obtained by dividing the axial load of the column by the area of the column section. Relations of axial stress verse axial displacement are shown in Fig.3-6. Result shows that the axial stress-displacement curves after yielding stress can be classified into three types, including softening behavior, elastic-perfectly-plastic behavior and strain hardening behavior [12].

Fig.3 shows the axial stress-displacement curve for specimens 400- F_c -31. It was found that specimen with a low strength concrete exhibited a lower ultimate axial stress

compared with the specimen with high strength concrete. However, a more ductile behavior tends to be yielded in the specimen with a low strength concrete.

Fig. 4 shows the axial stress-displacement curve for specimens 490-*Fc*-31. An observation similar to that of specimens 400-*Fc*-31 was found, while it should be noted that specimens 490-*Fc*-31 exhibited a higher ultimate axial stress and a more ductile behavior due to a higher strength steel is employed. Fig. 3 and Fig. 4 may suggest that specimen with a higher strength concrete exhibited a higher ultimate axial stress but a more brittle behavior of the column. Higher strength steel could improve the ductility of the columns.

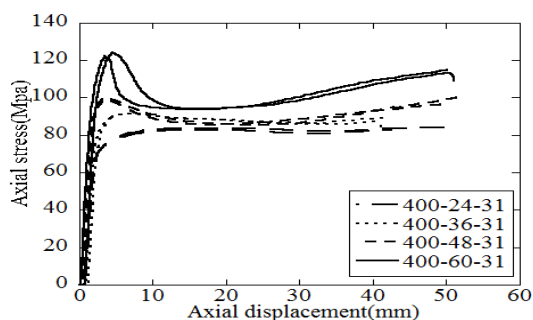


Fig. 3. Axial stress-displacement curve for specimens 400-*Fc*-31.

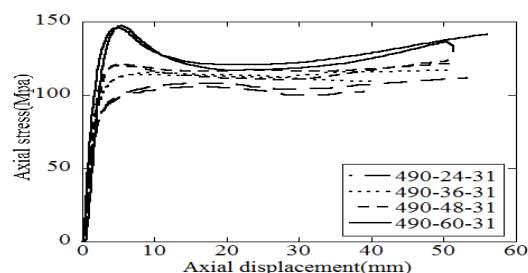


Fig. 4. Axial stress-displacement curve for specimens 490-*Fc*-31.

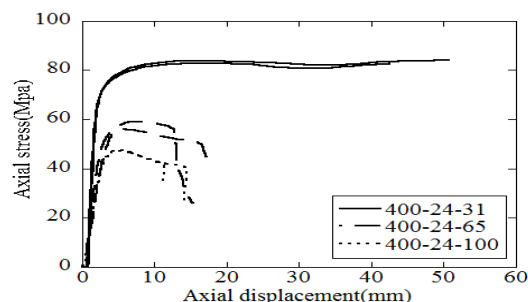


Fig. 5. Axial stress-displacement curve for specimens 400-24-*D/t*.

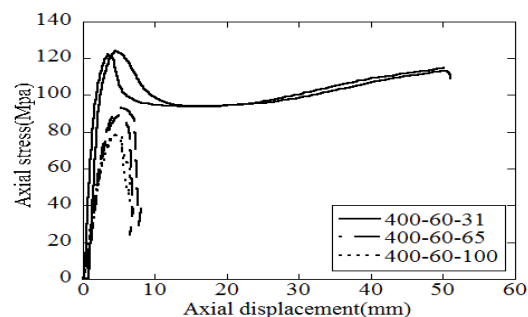


Fig. 6. Axial stress-displacement curve for specimens 400-60-*D/t*.

The axial stress-displacement curve for specimens 400-24-*D/t* and 400-60-*D/t* are shown in Fig. 5 and Fig. 6, respectively. Only the axial stress-displacement curve of

specimen 400-24-31 experienced a slight strain hardening behavior. It seems that specimen with a smaller *D/t* ratio tends to exhibit a higher ultimate axial stress and a more ductile behavior. As for thin-walled steel tube filled with high strength concrete, the axial stress-displacement curve of the column showed a drastic drop after reaching the yield strength.

B. Investigation on the Stress of the Steel Tube

In this section, the ultimate stresses of the steel tube in CFT columns are investigated.

Axial stress and hoop stress of the steel tube are normalized with respect to the yield stress f_y :

$$\alpha = \frac{\sigma_z}{f_y}; \beta = \frac{\sigma_\theta}{f_y} \quad (8)$$

Substituting Eq. (8) for Eq. (1), we have:

$$\omega = \sqrt{\alpha^2 - \alpha\beta + \beta^2} \quad (9)$$

where ω is the normalized equivalent stress with respect to the yield stress of the steel tube.

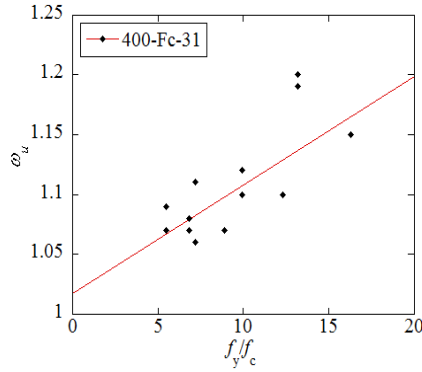
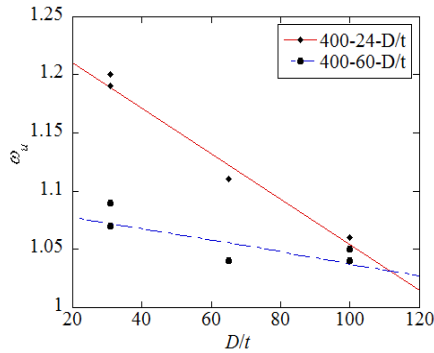
The axial stress and hoop stress at each loading step can be calculated by Eq. (1) - (7) from the strain of the steel tube measured from the strain gauge. Substituting the normalized axial stress and hoop stress for Eq. (9) obtained the normalized equivalent stress ω . The equivalent stresses of the steel tubes at the ultimate state of the columns are all summarized in TABLE II.

Influence of the strength ratio f_y/f_c and *D/t* ratio on the normalized ultimate stresses of the steel tube in CFT columns are shown in Fig. 7 and Fig. 8. It was found that the normalized ultimate stress of the steel tube increases with the strength ratio f_y/f_c , while decreases with the *D/t* ratio. That is, a higher degree of strain hardening behavior generally occurs in the specimen with a higher strength ratio f_y/f_c and/or a lower *D/t* ratio. However, it should be noted that influence of *D/t* ratio on the normalized ultimate stress (or degree of strain hardening) of the steel tube becomes less significant for the specimens with higher concrete strength.

TABLE II: RESULTS OF THE EXPERIMENTAL TEST

Specimen	<i>D</i> /mm	<i>t</i> /mm	f_y /Mpa	f_c /Mpa	N_u /kN	ω_u
400-24-31a	140	4.5	374.2	28.4	1275.3	1.20
400-24-31b	140	4.5	374.2	28.4	1287.8	1.19
400-36-31a	140	4.5	374.2	37.6	1406.4	1.10
400-36-31b	140	4.5	374.2	37.6	1409.3	1.12
400-48-31a	140	4.5	374.2	52	1524.3	1.06
400-48-31b	140	4.5	374.2	52	1530.4	1.11
400-60-31a	140	4.5	374.2	68	1880.9	1.07
400-60-31b	140	4.5	374.2	68	1910.0	1.09
490-24-31a	140	4.5	462.9	28.4	1625.5	1.15
490-24-31b	140	4.5	462.9	28.4	1662.3	1.15
490-36-31a	140	4.5	462.9	37.6	1771.1	1.10
490-36-31b	140	4.5	462.9	37.6	1753.8	1.10
490-48-31a	140	4.5	462.9	52	1865.2	1.07
490-48-31b	140	4.5	462.9	52	1850.6	1.07
490-60-31a	140	4.5	462.9	68	2268.3	1.08
490-60-31b	140	4.5	462.9	68	2247.7	1.08
400-24-65a	208	3.2	360.8	32	1901.8	1.11
400-24-65b	208	3.2	360.8	32	2010.5	1.11
400-24-100a	230	2.3	360.8	32	1973.8	1.05

400-24-100b	230	2.3	360.8	32	1963.5	1.04
400-60-65a	208	3.2	360.8	64	3172.9	1.06
400-60-65b	208	3.2	360.8	64	3040.1	1.06
400-60-100a	230	2.3	360.8	64	3272.5	1.05
400-60-100b	230	2.3	360.8	64	3263.8	1.05


 Fig. 7. Relation between ω_u and f_y/f_c .

 Fig. 8. Relation between ω_u and D/t .

As discussed above, the normalized ultimate stress of the steel tube is influenced by the parameters of the CFT column, such as concrete strength, steel strength and D/t ratio. To determine the normalized ultimate stress, a confinement coefficient including all the parameters are defined as:

$$\eta = \frac{2t}{D-2t} \frac{f_y}{f_c} \quad (10)$$

where D is the diameter of the column; t is the thickness of the steel tube.

Fig. 9 shows the relation between the normalized ultimate stress of the steel tube and the confinement coefficient. It was found that the normalized ultimate stress basically increases linearly with the confinement coefficient. That is, the steel tube tends to be more fully used in the specimen with a higher confinement coefficient. A model for the normalized ultimate stress of the steel tube is proposed as:

$$\omega_u = 0.12\eta + 1.03, \omega_u \leq \omega_t \quad (11)$$

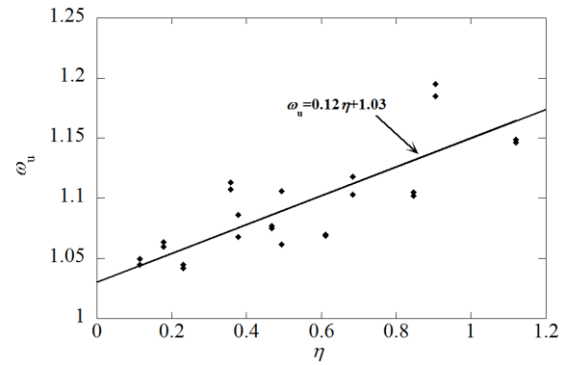
where ω_t is the normalized tensile strength of the steel.

The normalized tensile strength of the steel proposed by Tao [20] is adopted in this paper, which is given as:

$$\omega_t = \begin{cases} 1.6-2.00 \times 10^{-3}(f_y - 200), & 200 \leq f_y \leq 400 \\ 1.2-3.75 \times 10^{-4}(f_y - 400), & 400 < f_y \leq 800 \end{cases} \quad (12)$$

It should be noted that the ultimate strength of the steel tube in a CFT column is generally less than the tensile strength of the steel due to the local buckling of the steel tube. Therefore,

the normalized ultimate strength of the steel tube would be taken as the normalized tensile strength of the steel when the normalized ultimate strength of the steel tube determined by Eq. (11) exceeds the normalized tensile strength of the steel determined by Eq. (12).


 Fig. 9. Relation between ω_u and η .

The results predicted by the proposed model are compared with the experimental results. The mean and CoV of the ratios of the results predicted by the proposed model to the experimental results are 1.00 and 0.02, respectively. These suggested the ultimate stress of the steel tube in a CFT column can be accurately predicted by Eq. (11). Thus, relation between the normalized axial stress and hoop stress of the steel tube at the ultimate state of CFT column is then given as:

$$\sqrt{\alpha_u^2 - \alpha_u \beta_u + \beta_u^2} = \omega_u \quad (13)$$

where α_u and β_u are the normalized ultimate axial stress and hoop stress of the steel tube, respectively, and ω_u is the normalized ultimate equivalent stress of the steel tube, which is determined by Eq. (11).

IV. CONCLUSION

In this paper, experimental tests were conducted to investigate the ultimate stresses of the steel tubes in CFT stub columns. Based on the investigation, it was found that the stress of steel tube was influenced by the parameters of the columns, such as concrete strength, steel strength, and D/t ratio. Steel tube in the specimen with a higher strength ratio f_y/f_c and/or a smaller D/t ratio generally exhibits a higher degree of strain hardening behavior, which indicates a higher utilization efficiency of the steel tube. A model was proposed to predict the ultimate stress of the steel tube in a CFT stub column subjected to axial compression. The excellent performance of the proposed model is verified by comparison of the results predicted by the proposed model with the experimental results.

REFERENCES

- [1] S. Morino and K. Tsuda, "Design and construction of concrete-filled steel tube column system in Japan," *Earthquake Engineering and Engineering Seismology*, vol. 4, no. 1, pp. 51-73, Jan. 2003.
- [2] Z. B. Wang, Z. Tao, L. H. Han, B. Uy, D. Lam, and W. Hee Kang, "Strength, stiffness and ductility of concrete-filled steel columns under axial compression," *Engineering Structures*, vol. 135, pp. 209-221, 2017.

- [3] L. H. Han, X. L. Zhao, and Z. Tao, "Tests and mechanics model for concrete-filled SHS stub columns, columns and beam-columns," *Steel and Composite Structures*, vol. 1, no. 1, pp. 51-74, 2001.
- [4] S. P. Schneider, "Axially loaded concrete-filled steel tubes," *J. Struct. Eng.*, vol. 124, pp. 1125-1138, 1998.
- [5] M. D. O'Shea and R. Q. Bridge, "Design of circular thin-walled concrete filled steel tubes," *J. Struct. Eng.*, vol. 126, pp. 1295-1303, 2000.
- [6] K. Sakino, H. Nakahara, S. Morino, and I. Nishiyama, "Behavior of centrally loaded concrete-filled steel-tube short columns," *J. Struct. Eng.*, vol. 130, pp. 180-188, 2004.
- [7] E. Ellobody, B. Young, and D. Lam, "Behaviour of normal and high strength concrete-filled compact steel tube circular stub columns," *J. Constr. Steel Res.*, vol. 62, pp. 706-715, 2010.
- [8] G. D. Hatzigeorgiu, "Numerical model for the behavior and capacity of circular CFT columns, Part I: theory," *Eng. Struct.*, vol. 30, pp. 1573-1578, 2008.
- [9] P. K. Gupta, S. M. Sarda, and M. S. Kumar, "Experimental and computational study of concrete filled steel tubular columns under axial loads," *Journal of Constructional Steel Research*, vol. 63, pp. 182-193, 2007.
- [10] M. M. El-Heweity, "On the performance of circular concrete-filled high strength steel columns under axial loading," *Alexandria Engineering Journal*, vol. 51, pp. 109-119, 2012.
- [11] Z. W. Yu, F. X. Ding, and C.S. Cai, "Experimental behavior of circular concrete-filled steel tube stub columns," *Journal of Constructional Steel Research*, vol. 63, pp. 165-174, 2007.
- [12] M. Johansson, "The efficiency of passive confinement in CFT columns," *Steel and Composite Structures*, vol. 2, no. 5, pp. 379-396, 2002.
- [13] W. L. A. D. Oliveira, S. D. Nardin, A. L. H. D. C. E. Debs, and M. K. E. Debs, "Evaluation of passive confinement in CFT columns," *Journal of Constructional Steel Research*, vol. 66, pp. 487-495, 2010.
- [14] H. B. Ge and T. Usami, "Strength analysis of concrete-filled thin-walled steel box columns," *Journal of Constructional Steel Research*, vol. 30, pp. 607-612, 1994.
- [15] H.T. Hu, C. S. Huang, M. H. Wu, and Y. M. Wu, "Nonlinear analysis of axially loaded concrete-filled tube columns with confinement effect," *J. Struct. Eng.*, vol. 129, pp. 1322-1329, 2003.
- [16] K. K. Choi and Y. Xiao, "Analytical studies of concrete-filled circular steel tubes under axial compression," *J. Struct. Eng.*, vol. 136, pp. 565-573, 2010.
- [17] M. H. Lai and J. C. M. Ho, "Behaviour of uni-axially loaded concrete-filled-steel-tube columns confined by external rings," *Struct. Design Tall Spec. Build.*, vol. 23, pp. 403-426, 2014.
- [18] K. Masanori, P. N. Milija, and D. K. Michael, "Constitutive models of concrete under passive confinement and their use in structural analysis," *J. Materials Conc. Struct., Pavements*, no. 502/V-25, pp. 143-154, Nov. 1994.
- [19] S. T. Zhong, "The concrete filled steel tubular structures," third ed., Beijing: Tsinghua University Press, 2003, pp. 34-48.
- [20] Z. Tao, Z. B. Wang, and Q. Yu, "Finite element modelling of concrete-filled steel stub columns under axial compression," *Journal of Constructional Steel Research*, vol. 89, pp. 121-131, 2013.



Siqi Lin was born in Fujian, China in 1989. He received the B.S. degree of project management in 2008 and M.S. degree of civil engineering in 2012 from the North China University of Technology. He is a Ph.D. candidate in Kanagawa University.



Yan-gang Zhao was born in Shandong, China in 1963. He received the Ph.D. degree in 1996 from the Nagoya Institute of Technology. He is a professor in Kanagawa University.